MICROSTRUCTURE CHANGES OF P92 WELD DURING CREEP EXPOSURE

Petr MOHYLA[a], Kristýna STERNADELOVÁ[a], Miroslav LINDOVSKÝ[a], Jiřina VONTOROVÁ[b]

[a] *Flash Steel Power, a.s., Ostrava, Czech Republic, EU, p.mohyla@flashsteel.cz*

[b] *VSB-Technical University of Ostrava, FMMI, Ostrava, Czech Republic, EU*

Abstract

This work is a contribution to the research of modified heat resistant steel P92. This steel is currently one of the best modified chromium steels in terms of achieved values of creep rupture strength. The article is focused on microstructure investigation of P92 weld after creep deformation. Up to date results of creep rupture test of P92 welds are presented here too. The microstructure in the as welded condition and after long-term creep exposure (26.000 hours/600 °C) of P92 welds has been investigated and microstructural parameters were determined. Results of intercritical zone of heat affected zone (HAZ) are compared with parameters of parent material, which is not influenced by welding. Results of TEM analyses reveal deteriorating effect of welding procedure on microstructure od P92 welds during subsequent creep exposure.

Keywords: P92 Weld, Heat Affected Zone, Intercritical Zone, Microstructure, Creep Properties, TEM Analysis, Laves Phase

1. INTRODUCTION

Efforts to increase the efficiency of power plants and improving of the environment is the driving force in the development of modern power plants. Economic requirements for beneficial use of fossil fuels and reducing of carbon dioxide emissions lead to a constant increase in thermal efficiency of power plants. The current target for coal power plants is to increase the thermal efficiency from 42% to 45%. This can be achieved by increasing the temperature and pressure of steam above 600°C/30 MPa. Using USC parameters can reduce carbon dioxide emissions by about 20% [1].

It is therefore necessary to develop new high-chromium ferritic steels with improved creep properties and sufficient resistant to oxidation in water vapor at temperatures exceeding 600 °C. For these operating temperatures were developed new 9-12% chromium martensitic steels. Firstly, there was developed a modified 9% Cr, designated P91. Further development brings alloying of steels by tungsten. Typical representatives of modified chrome steel with tungsten are steels E911 and P92.

The original estimates of creep rupture strength of steel P92, based on short-term creep tests, were about 190 MPa at 600 °C for 100.000 hours. Recent research based on long-term creep tests resulted in settlement of CRS about 110 MPa at 600 °C for 100.000 hours [2, 3]. In comparison with other ferritic creep resistant steels it is still high value.

High creep resistance of steel P92 is done especially by precipitation of vanadium nitrides. These very finely dispersed and stable particles effectively prevent the movement of dislocations and thereby slow down the creep rate. In addition to dispersion hardening a solid solution strengthening is involved in high creep resistance of steel P92. This is due to substitution elements Mo and W dissolved in the solid solution. The latest research shows that nitrogen and especially boron is essential to achieve high creep rupture strength of steel P92. It has been shown that P92 steel without boron has low values of creep rupture strength, even lower than steel P91 (containing 9% Cr, 1% Mo, 0.2% V, 0.05% Nb and about 0.05% N) [3]. Positive affect of nitrogen on heat resistant properties was observed in the content up to 0.08% [3].

2. EXPERIMENTAL MATERIAL

Testing welded joint made by manual metal arc welding (MMAW) were used for further experiments. Chemical composition of parent material is shown in **Table 1**. Consumables used for welding were covered electrodes Thermanit MTS 616 (EN 1599:E Z CrMoWVNb 9 0,5 2 B 4 2H5), see **Table 2**.

Table 1 Chemical composition of experimental base material - steel P92

C	Mn	Si	Cr	Mo	V	W	Ni	Nb	Al	N
0.090	0.50	0.34	8.85	0.50	0.21	1.90	0.31	0.084	0.008	0.0595

Table 2 Chemical composition of covered electrodes used for experimental welded joint

C	Si	Mn	Cr	Mo	Ni	W	V	Nb	N
0,11	0,2	0,6	8,8	0,5	0,7	1,6	0,2	0,05	0,05

3. CREEP TESTS

Parent material and welded joint of P92 steel were tested in extensive experimental program of creep rupture tests. Solid line in **Fig. 1** represents standardized values, dashed line represents allowed -20% scattering band for base material and dotted line represents allowed -40% scattering band for welds. Open symbols represent running tests.

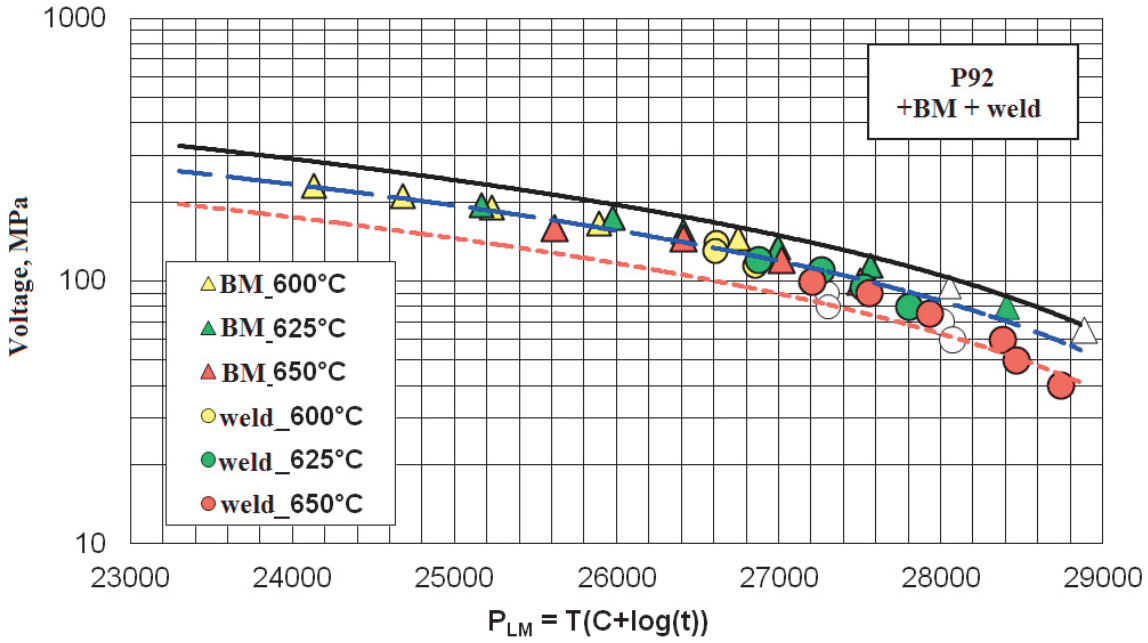

Fig. 1 Dependence of stress on the value of Larson-Miller parameter for assessing welded joints, the base material and standardized mean values of steel P92

Results of base material creep tests show that the experimental results lie in allowed -20% scattering band. With the increasing value of the LM parameter (and thus extending the time to fracture), experimental results tend to be closer to the mean standardized value. Creep strength of weld joints is almost the same like creep strength of the base material. With increasing time to fracture, especially at higher temperatures, the creep strength of welded joint decreases and the data are closer to the allowed -40% scattering band.

4. MICROSTRUCTURAL ANALYSIS

In the first instance there has been analyzed a sample of the weld without creep exposure. In the second step of an experimental program there has been analyzed a sample of the weld after creep exposure (25.861 hours at 600 °C). TEM analyses were performed in particular areas of the welded joint.

5. RESULTS

5.1 Weld before creep

The microstructure of all examined specimens was consisting of tempered martensite with a high dislocation density and finely distributed carbides or carbonitrides. The dominant precipitated particles were the $M_{23}C_6$ carbides. These precipitates were located mainly at prior austenite grain boundaries and at sub-grain boundaries however they also appear within martensite laths. In addition, three types of MX precipitates were present: fine spheroidal Nb-rich carbonitride, plate-like V-rich nitride and complex "V-wings" (Nb(C,N)-VN). In **Fig. 2** are TEM micrographs of intercritical zone of HAZ. **Table 3** presents results of dislocation density and equivalent circular diameter (ECD) of $M_{23}C_6$ and MX particles.

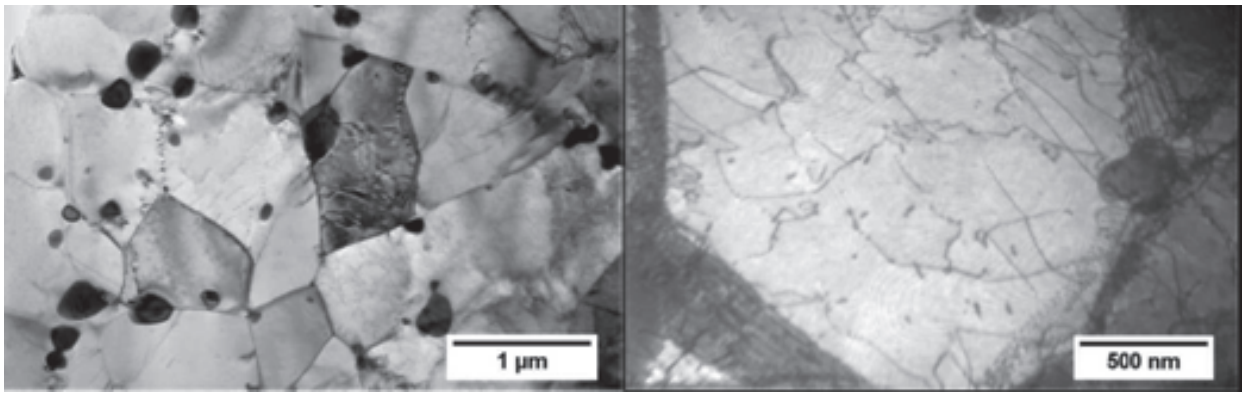

Fig. 2 TEM micrographs of intercritical heat affected zone, left: Typical morphology of $M_{23}C_6$ carbides, right: carbonitrides MX inside sub-grain

Table 3 Dislocation density and ECD of $M_{23}C_6$ and MX in the weld before creep deformation

Region	Dislocation density [10^{14} m^{-2}]	ECD of $M_{23}C_6$ [nm]	ECD of MX [nm]
Base material	3.68	120	27.6
Intercritical zone of HAZ	1.82	140	32.5
Coarse grained zone of HAZ	2.49	110	30.4

In the sample before creep exposition the equivalent circle diameter (ECD) of $M_{23}C_6$ carbides was in the range of 110 - 140 nm. The largest carbides were observed in the intercritical zone (140 nm). Moreover, in this zone the lowest dislocation density was observed (1,82x10^{14} m^{-2}). This means that the weakest part of the weld in terms of creep resistance is precisely intercritical zone.

The highest dislocation density was observed in base material (3,68x10^{14} m^{-2}). The size of MX carbonitrides was in the range of 30 nm in all specimens. Results **Table 3** summarizes.

5.2 Weld after creep exposure

For microstructural investigatons there was chosen a sample which ruptured after 25.861 hours at 600°C and 105 MPa. The fracture occurred in the intercritical heat affected zone, see **Fig. 3**. Red line characterizes the

fusion line. In the intercritical heat affected zone on the opposite side of the weld, there was observed the neck creation, see **Fig. 4**.

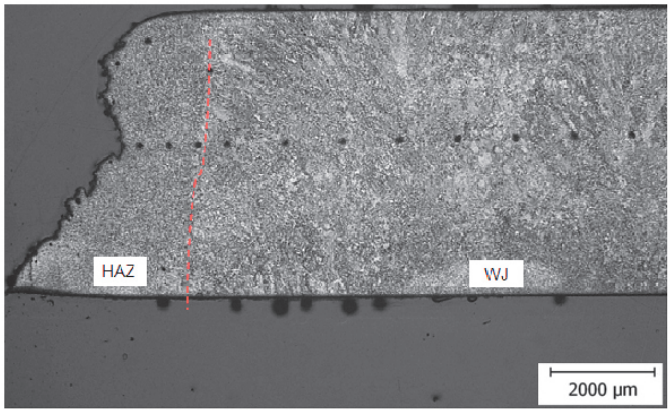

Fig. 3 The fracture in the intercritical heat affected zone

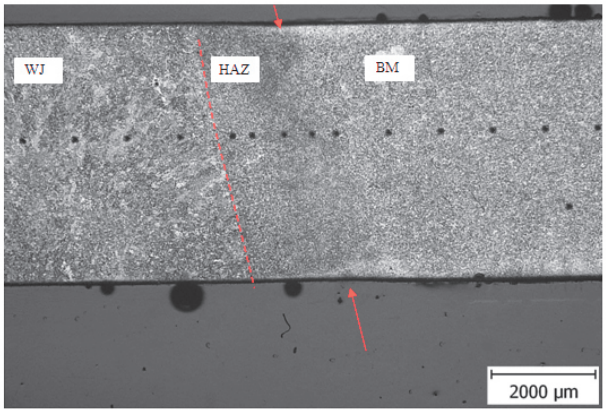

Fig. 4 Intercritical heat affected zone on the opposite side of the weld

During creep exposure there was observed significantly cavitation damage especially in the intercritical heat affected zone, see **Fig. 5**. Typical microstructure of base material is composed of tempered martensite without delta ferrite, see **Fig. 6**.

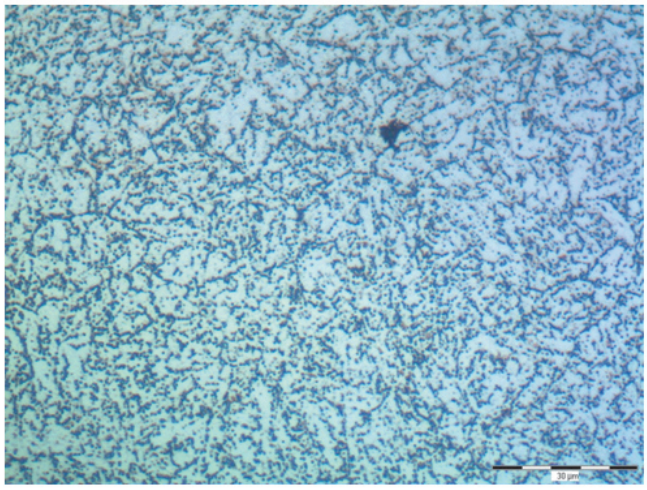

Fig. 5 Microstructure and cavitations in the intercritical heat affected zone

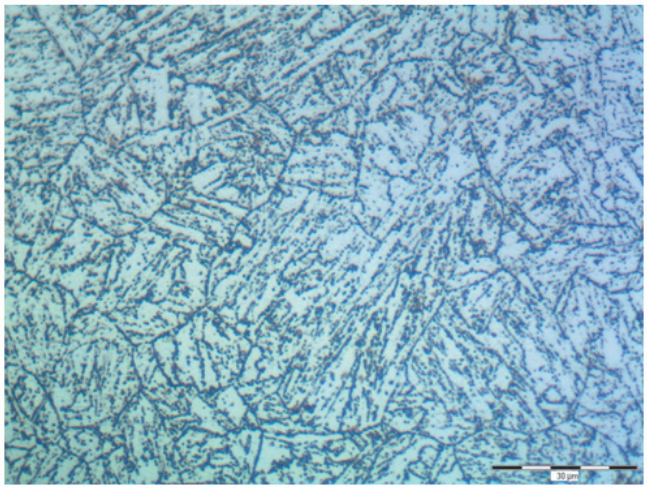

Fig. 6 Typical microstructure of base material

Study of precipitation in the weld after creep deformation was performed using the carbon extraction replicas. Replicas were prepared from the following areas of weldment: base material, weld metal and intercritical heat affected zone (the softest part of the welded joint). Precipitation in intercritical heat affected zone is documented in **Fig. 7**. Using EDX analyze there were identified following minor phase: ultra-fine particles MX, medium-sized carbides $M_{23}C_6$, and large particles of Laves phase (Fe_2W type).

The mean particle size of secondary phases was highly variable (MX particles reached usually several tens of nanometers, while Laves phase reached up to several hundred of nanometers).

Laves phase particles nucleated during creep exposure, were usually found along the grain or sub-grain boundaries (heterogeneous nucleation). The nucleation of Laves phase particles occurred gradually and therefore the size of the individual particles of this phase depended on the time required for their nucleation (the coarsest particles nucleated first). Distribution of Laves phase particles in the intercritical heat affected zone is shown in **Fig. 8**.

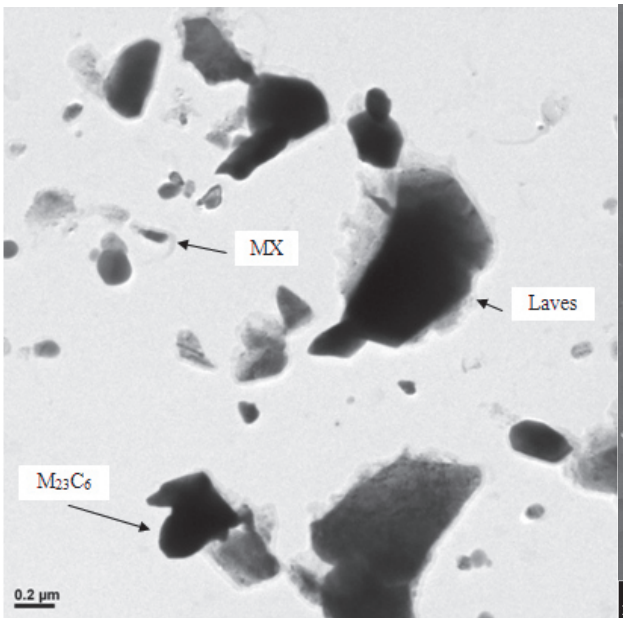

Fig. 7 Precipitation in the intercritical heat affected zone

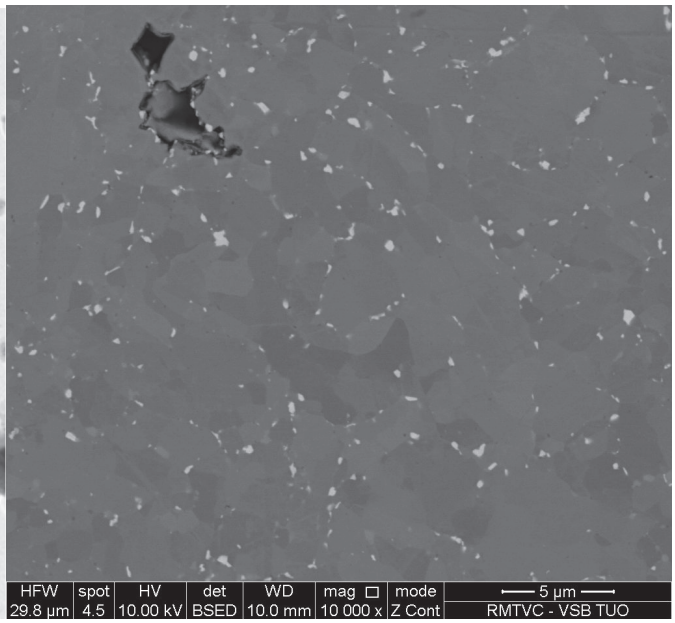

Fig. 8 Distribution of Laves phase particles (bright contrast) in the intercritical affected zone

It is evident that some of the Laves phase particles reach a size of up to 1000 nm. Quantification of precipitation in each of the studied areas was performed on carbon replicas using automated image analysis.

Number of measured particles N in the individual areas of the weld was in the range of 700-900. In processing of results there were not considered objects with an equivalent circle diameter smaller than 15 nm. The largest mean particle size of precipitates was found in the intercritical heat affected zone, the smallest mean equivalent diameter (ECD) was measured in the weld metal. The minimum number of particles per unit area N_A was found in the intercritical heat affected zone - see **Table 4**.

Table 4 Results of image analysis of the precipitates in the weld after creep exposure

Region	ECD [nm]	D_{max} [nm]	D_{min} [nm]	N	N_A [mm^{-2}]
Base material	96 ± 75	862	6	890	2,4 x 10^6
Weld metal	83 ± 75	753	5	734	1,98 x 10^6
Intercritical zone	124 ± 109	1167	6	811	1,3 x 10^6

6. DISCUSSION

The smallest mean particle size of the precipitate was observed in the weld metal. Unlike the base material the weld metal has not been subjected to tempering below A_1 temperature, which leads to significant particle growth of the precipitate, mainly $M_{23}C_6$ particles.

The largest mean equivalent diameter of the precipitates was observed in the intercritical heat affected zone of HAZ. In this area occurred partial re-austenitizing during welding accompanied by redistribution of carbon in austenite and secondly by partial dissolution of the precipitates present in the base material. After cooling of the weld there formed significant microstructural and chemical heterogeneity in this area. Local differences in hardness across the weld led to the concentration of plastic deformation during creep in the intercritical heat affected zone, especially in locations that remain ferritic during intercritical annealing. As a result of partial dissolution of precipitates in these areas are accelerated processes of recovery and recrystallization of the metal matrix. The creep deformation also accelerates the processes of growth and coarsening of precipitates, which are controlled by diffusion. That is why is reasonable that mean dimensions of precipitates in the intercritical heat affected zone is larger than in other parts of the welded joint.

CONCLUSIONS

Steel P92 is considered to be one of the best martensitic creep resistant steel in terms of achieved values of creep rupture strength. Presented creep tests of investigated heat confirmed its satisfactory creep resistance. Creep strength of investigated weld is comparable with creep strength of the base material. With increasing time to fracture, especially at higher temperatures, the creep strength of welded joint significantly decreases, which is expected result.

Micro-mechanism of damage of the weld after creep deformation corresponds to the IV. type of failure - in the intercritical heat affected zone of HAZ. This is the predominant mechanism of damage of homogeneous welded joints in the case of relatively low applied strength.

Results of the experiment confirmed that Intercritical heat affected zone is the weakest part of investigated welded joint in terms of creep resistance. Deteriorating effect of welding procedure on microstructure of P92 welds during subsequent creep exposure is therefore evident.

ACKNOWLEDGEMENTS

This work presented in this article was supported by the Ministry of Industry and Trade of Czech Republic in the frame of the project FR-TI3/206.

REFERENCES

[1] MAYER, K. H., KERN, T. U., STAUBLI, M. E. *Stand der Entwicklung moderner thermischer Energieerzeugsanlagen unter Berücksichtigung der eingesetzten Werkstoffe.* In Werkstoffe für Kraftwerkstechnik an der Schwelle zur 21. Jahrhundert, TU Graz 1999.

[2] *ECCC DATA SHEETS 2005*, September 2005.

[3] FOLDYNA, V. et al. Development of Advanced Creep Resistant Ferritic Steels and their Weldability. In: *Proceedings of conference Progresívne kovové materiály a ich spájanie. 2004*, Bratislava.